*Journal of Experimental Botany*, Vol. 60, No. 11, pp. 3023–3030, 2009
doi:10.1093/jxb/erp133 Advance Access publication 12 May, 2009

Journal of Experimental Botany
www.jxb.oxfordjournals.org

RESEARCH PAPER

# Mesoporosity as a new parameter for understanding tension stress generation in trees

**Shan-Shan Chang[1,2], Bruno Clair[1,*], Julien Ruelle[3], Jacques Beauchêne[4], Francesco Di Renzo[5], Françoise Quignard[5], Guang-Jie Zhao[2], Hiroyuki Yamamoto[3] and Joseph Gril[1]**

[1] Laboratoire de Mécanique et Génie Civil (LMGC), Université Montpellier 2, CNRS, Pl. E. Bataillon, cc 048, 34095 Montpellier Cedex 5, France
[2] College of Materials Science and Technology, Beijing Forestry University, Beijing, 100083, PR China
[3] School of Bioagricultural Sciences, Nagoya University, Chikusa, Nagoya 464-8601, Japan
[4] Ecologie des Forêts de Guyane (EcoFoG), CIRAD, BP 709, 97387 Kourou cedex, French Guyana
[5] Institut Charles Gerhardt Montpellier,UMR 5253 Université Montpellier 2, CNRS, ENSCM, UM1, 8 rue Ecole Normale, 34296 Montpellier Cedex 5, France

Received 18 November 2008; Revised 31 March 2009; Accepted 5 April 2009

## Abstract

**The mechanism for tree orientation in angiosperms is based on the production of high tensile stress on the upper side of the inclined axis. In many species, the stress level is strongly related to the presence of a peculiar layer, called the G-layer, in the fibre cell wall. The structure of the G-layer has recently been described as a hydrogel thanks to $N_2$ adsorption–desorption isotherms of supercritically dried samples showing a high mesoporosity (pores size from 2–50 nm). This led us to revisit the concept of the G-layer that had been, until now, only described from anatomical observation. Adsorption isotherms of both normal wood and tension wood have been measured on six tropical species. Measurements show that mesoporosity is high in tension wood with a typical thick G-layer while it is much less with a thinner G-layer, sometimes no more than normal wood. The mesoporosity of tension wood species without a G-layer is as low as in normal wood. Not depending on the amount of pores, the pore size distribution is always centred around 6–12 nm. These results suggest that, among species producing fibres with a G-layer, large structural differences of the G-layer exist between species.**

**Key words:** Growth stress, hydrogel, mesoporosity, tension wood.

## Introduction

Tension wood (TW) is a peculiar wood tissue that is often formed in the upper side of leaning trunks and branches in hardwood species (Isebrands and Bensend, 1972) to control the orientation of the growth axis by generating high tensile stress (Wardrop, 1964; Fisher and Stevenson, 1981). For many commonly studied species such as beech, poplar, oak, or chestnut, TW is characterized by the occurrence of fibres with a particular morphology and chemical composition due to the development of the so-called gelatinous layer (G-layer). This layer is composed of cellulosic microfibrils that are nearly parallel to the fibre axis (Dadswell and Wardrop, 1955; Wardrop, 1964; Côté *et al.*, 1969) embedded in a highly hydrated polysaccharide matrix (Nishikubo *et al.*, 2007; Bowling and Vaughn, 2008; Mellerowicz *et al.*, 2008).

Although it has been well established that the G-layer is the driving force of the high tensile stress generated in TW (Trénard and Guéneau, 1975; Yamamoto *et al.*, 2005; Fang *et al.*, 2008), the underlying mechanism is still a subject of debate. In previous research, the structure of the G-layer has been described as possessing gel-like characteristics: large shrinkage (Clair and Thibaut, 2001; Fang *et al.*, 2007) and high rigidification during drying (Clair *et al.*, 2003). Recently, the hydrogel structure of the chestnut G-layer has been characterized thanks to nitrogen adsorption. The

* To whom correspondence should be addressed: E-mail: clair@lmgc.univ-montp2.fr

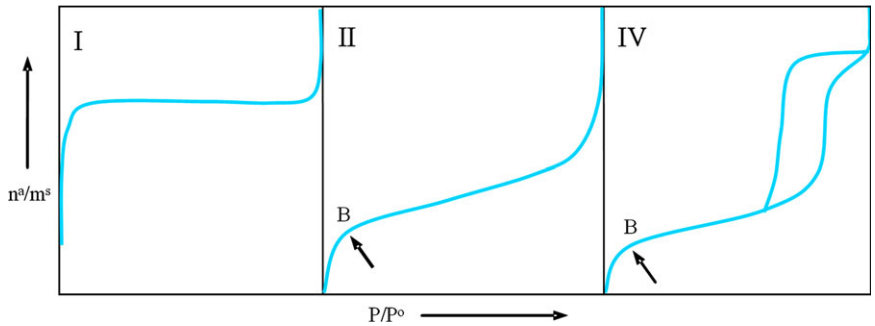


**Fig. 1.** The three types of adsorption isotherms usually found by nitrogen adsorption [types I, II, and IV by IUPAC classification; reprinted from Sing *et al.* (1985), with kind permission from IUPAC]. $P/P^0$: relative pressure; $n^a/m^s$: quantities adsorbed $g^{-1}$ sample expressed as mmol $g^{-1}$.

chestnut G-layer contains mesopores (pore size between 2 nm and 50 nm) and the pore surface areas is more than 30 times higher than that in normal wood (NW) (Clair *et al.*, 2008). The swelling of the G-layer matrix has been suggested recently by several authors as the possible driving force of the growth stress generation in TW (Nishikubo *et al.*, 2007; Goswami *et al.*, 2008). However, it is known that many species (Onaka, 1949; Fisher and Stevenson, 1981; Clair *et al.*, 2006) are able to produce tensile stress without forming a typical G-layer. Different anatomical patterns of TW exist, from fibres with a typical G-layer to fibres exhibiting no difference at the fibre level (Clair *et al.*, 2006; Ruelle *et al.*, 2006, 2007).

These results led us to revisit the concept of the G-layer and to propose an objective description of the TW cell wall structure, until now only defined from visual assessments (stain, detachment or swollen aspect) which are the subject of much debate (Clair *et al.*, 2005*a*, *b*, 2006).

Let us briefly introduce the principles of mesoporosity measurements by the nitrogen adsorption method. This technique, based on the measurement of the adsorption isotherm of nitrogen at its boiling temperature (77 K) on an outgassed sample, allows the pore size and surface area of materials with cavities smaller than 50 nm to be estimated (Gregg and Sing, 1982; Rouquerol *et al.*, 1999) and has recently been applied to the study of the texture of polysaccharide aerogels (Valentin *et al.*, 2005; Quignard *et al.*, 2008). The majority of isotherms have been grouped into six types by IUPAC classification (Sing *et al.*, 1985), but only three are commonly found in the adsorption on polar materials (type I, type II, and type IV in Fig. 1).

Type I is obtained with microporous (pore size <2 nm) solids. The adsorption takes place at very low relative pressure regions (the ratio between pressure and saturation pressure $P/P°$ <0.3) because of multidirectional interactions between the pore walls and the adsorbate. The reversible type II isotherm is characteristic of the non-porous or macroporous (pore size >50 nm) solids. If the knee of the isotherm is sharp, the uptake at point B—the beginning of the middle linear section—provides a measure of the monolayer capacity, from which the surface area of the adsorbent can be calculated. The type IV isotherm is obtained with mesoporous (2 nm <pore size <50 nm) solids. The hysteresis

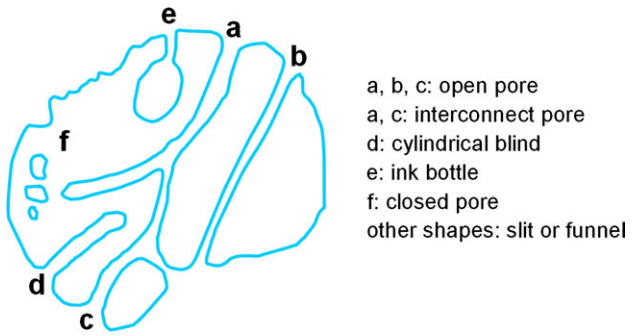


**Fig. 2.** Physical picture of porous solid. Reprinted from Rouquerol *et al.* (1999), with kind permission from Elsevier.

loop is associated with the secondary process of capillary condensation, which results in the complete filling of the mesopores at $P/P°$ <1.

Pores can have a regular or, more commonly, an irregular shape, either an ink-bottle shape (pore body larger than pore mouth) or a funnel shape (the opposite). Pores can be closed (not accessible from the outside), blind (open only at one end), or through (open at both ends). Each pore can be isolated or, more frequently, connected to other pores to form a porous network (Rouquerol *et al.*, 1999) (Fig. 2). The surface and structural properties of the pores control the interactions of material with gases, fluids, and other solids.

The adsorbate desorption is the opposite of adsorption, but evaporation from mesopores usually takes place at a pressure lower than that of capillary condensation giving a hysteresis loop. The reason for the hysteresis is that the formation of the meniscus in capillary condensation is an activated phenomenon, while the retreat of the meniscus in evaporation is usually an equilibrium phenomenon. Pore shape affects the mechanisms of condensation and evaporation and four types of hysteresis have been recognized according to IUPAC classification (Sing *et al.*, 1985) (Fig. 3).

Type H1 hysteresis is characteristic of solids crossed by channels with uniform sizes and shapes. Type H2 corresponds to channels with a pore mouth smaller than the pore body (this is the case of ink-bottle-shaped pores). Type H3

hysteresis is usually found on solids with a very wide distribution of pore size and type H4 corresponds to limited amounts of mesopores limited by micropores.

The aim of this study was to adapt experimental techniques used in material chemistry to the specificity of biological material such as wood. It was applied to tension wood of several angiosperm species to answer the following questions: is the occurrence of a G-layer always associated with high porosity? Does non-G-layer TW contain mesopores? Do all TW types have the same pore shape and pore size distribution? Can we check the presence/absence of the G-layer by an $N_2$ adsorption–desorption isotherm?

## Materials and methods

Experiments were performed on six tropical rainforest species (one tree per species) distributed in three families (Table 1). Sampling was carried out near the Paracou experimental field in French Guyana. Care was taken to maintain the samples in wet conditions in storage from the living tree to the experiments. TW occurrence was demonstrated by the mechanical measurement of released strains at the circumference of the leaning trees.

### *Growth stress measurements*

The strain gauge method (Yoshida and Okuyama, 2002; Jullien and Gril, 2008) was used to estimate the residual growth stress close to the trunk surface on the living tree. Measurements of longitudinal growth strains (GS expressed in μm $m^{-1}$ or microstrain) were performed at eight positions every 45° around the circumference of the inclined trunks at breast height.

Tension stress gives a negative strain value while compression stress gives a positive strain value. A high local level of growth stress is always related to the presence at TW (Trénard and Guéneau, 1975). For each species, a TW sample was taken near the highest absolute value of growth stress, while a NW sample was taken near the lowest absolute value.

### *Anatomical observations*

Cross-sections (12 μm in thickness) were cut with a sliding microtome equipped with disposable razor blades. Double staining with safranin/fast green was used to demonstrate the presence of the G-layer. Safranin stains lignified tissues red, and fast green stains both lignified and unlignified cell walls green. Consequently, lignified tissues were red mixed with varying degrees of green while essentially cellulosic cell wall layers, like the G-layer, were green. Sections were observed with an optical microscope at ×400 magnification.

### *$N_2$ adsorption–desorption measurement*

As direct drying usually results in the collapse of mesoporosity (Clair *et al.*, 2008), samples were supercritically dried as follows.

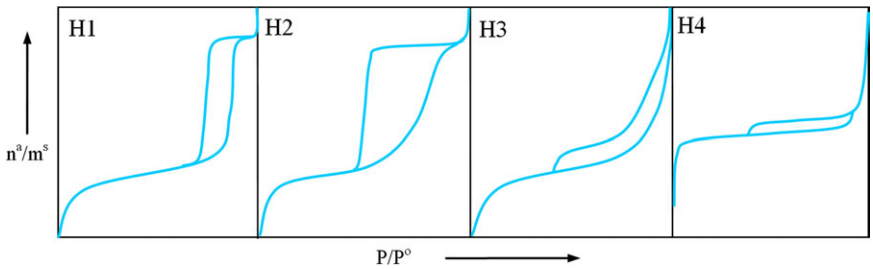


**Fig. 3.** The four hysteresis loops of adsorption isotherms by IUPAC classification [reprinted from Sing *et al.* (1985), with kind permission from IUPAC]. $P/P^0$, relative pressure; $n^a/m^s$, quantities adsorbed per gram sample expressed as mmol $g^{-1}$.

**Table 1.** Characteristics of the six species studied

GS, growth strain (μstrain); TW, tension wood; NW, normal wood; $V_{MP}$, mesopore volume; $S_{BET}$, specific surface area; $D_a$ ($D_d$), average mesopore diameter on adsorption (desorption) branch of the isotherm. Three types of wood fibre were classified according to the G-layer patterns: $G_{thin}$, with a thin G-layer; $G_{thick}$, with a thick G-layer; no G, G-layer absent. In *T. melinonii*, a thin G-layer was observed but it was sparse on the wood sample.

| Family | Species | Tree diameter (cm) | GS (μstrain) | | Fibre pattern | $V_{MP}$ ($cm^3\ g^{-1}$) | | $S_{BET}$ ($m^2\ g^{-1}$) | | Da (nm) | | Dd (nm) | |
|---|---|---|---|---|---|---|---|---|---|---|---|---|---|
| | | | TW | NW | | TW | NW | TW | NW | TW | NW | TW | NW |
| Lauraceae | *Ocotea guyanensis* | 19 | −2097 | −399 | $G_{thin}$ | 0.003 | <0.001 | 2.8 | 0.3 | 11 | – | 7 | – |
| Lauraceae | *Sextonia rubra* | 25 | −2362 | −328 | $G_{thick}$ | 0.133 | 0.002 | 64.6 | 2.6 | 7 | 9 | 6 | 6 |
| Fabaceae | *Inga alba* | 29 | −2408 | −310 | $G_{thin}$ | 0.014 | 0.016 | 8.8 | 11.9 | 6 | 9 | 6 | 8 |
| Fabaceae | *Tachigali melinonii* | 18 | −1488 | −480 | $G_{thin}$ | 0.004 | 0.001 | 4.8 | 1.7 | 9 | 11 | 8 | 12 |
| Myristicaceae | *Virola michelii* | 36 | −1708 | +45 | no G | 0.003 | 0.003 | 2.6 | 2.1 | 9 | 9 | 12 | 15 |
| Myristicaceae | *Iryanthera sagotiana* | 26 | −1485 | +12 | no G | 0.005 | 0.002 | 4.7 | 1.9 | 11 | 11 | 11 | 15 |

Wood sticks (5 mm in a longitudinal direction, 1×1 $mm^2$ in cross-section) were dehydrated by immersion in increasing concentrations (10, 30, 50, 70, 90, 100%, and anhydrous) of ethanol solutions for 3 d each. The dehydrated samples were then introduced into a Polaron 3100 apparatus which was filled with liquid $CO_2$. Samples were left for 2 h in liquid $CO_2$ before ethanol evacuation. The temperature was raised to 32 °C so that $CO_2$ reached its critical point (74 bar, 31.5 °C). Depressurization took 30 min. During this procedure the liquid phase has been transformed in a supercritical fluid with a null surface tension. In this way, the shrinkage due to capillary pressure was prevented and the solid obtained, an aerogel, was expected to reproduce the texture of the original hydrogel in the dry state (Pierre and Pajonk, 2002; Cansell *et al.*, 2003).

Nitrogen adsorption–desorption was performed on a micromeritics ASAP 2010 volumetric apparatus at 77 K. Before adsorption measurements, samples (1.0–1.5 g) were outgassed at 373 K under vacuum until a stable $3\times10^{-5}$ Torr pressure was obtained without pumping. This is done to remove physically absorbed gases from the sample surface, in particular, water vapour. The adsorption at low relative pressure allows the specific surface area of the samples to be evaluated by the BET method (Brunauer *et al.*, 1938), assuming an adsorbed $N_2$ molecule covers 0.162 $nm^2$. Pore size distributions calculated from adsorption and desorption data using the method of Broekhoff and de Boer, proved more accurate than the commonly used BJH method (Barrett *et al.*, 1951; Galarneau *et al.*, 1999). The pore volume was evaluated by the $\alpha_S$ method (Gregg and Sing, 1982) and is given in Table 1 by assuming for condensed $N_2$ the density of liquid $N_2$. The adsorbed volume in the figures is given as the volume of gas at standard temperature and pressure, with a density 647 times lower than the liquid density.

## Results

### Anatomical observations

Anatomical sections of TW and NW in the six species are illustrated in Fig. 4. *Ocotea guyanensis*, *Sextonia rubra*, *Tachigali melinonii*, and *Inga alba* TW have fibres with a well-differentiated G-layer that is obviously green after double staining with safranin/fast green (Fig. 4A, C, E, G). However, there are notable differences in morphology, thickness, and distribution. In TW fibres of *S. rubra*, a thick G-layer almost fills up the entire lumen, whereas in *O. guyanensis*, *I. alba* or *T. melinonii* TW, the G-layer is thinner, sometimes delaminated from the adjacent $S_2$ and folded into the lumen towards the same direction. This detachment phenomenon results from sample preparation with classical sectioning (Clair *et al.*, 2005*b*). In *T. melinonii*, a G-layer was only observed in a limited number of fibres whereas, in the other three species, most fibres contained a G-layer.

For the other two species (*Virola michelii* and *Iriantera sagotiana*) there is no G-layer and no obvious difference between TW and NW fibres can be seen simply by anatomical observation. Irrespective of the fibre pattern, all species can produce a high level of mechanical tensile stress (ranging from –2408 to –1485 μstrain). As already shown earlier (Clair *et al.*, 2006; Ruelle *et al.*, 2006), the general relations between tensile stress level in tension wood and macroscopic anatomical variations are not visible, while observation at an ultrastructural level allows some common features in cellulose organization to be seen (Ruelle *et al.*, 2006, 2007).

### Textural characterization

The textural parameters of TW and NW in six species are reported in Table 1. *S. rubra*, the only specimen with a thick G-layer, is the only one to present a TW with a very high mesopore volume. The other samples, with a thin G-layer or no observable G-layer, present a much lower mesopore volume difference between TW and NW.

### Pore surface area ($S_{BET}$)

Examples of nitrogen adsorption–desorption isotherms (77 K) of *S. rubra* and *I. sagotiana* are shown in Fig. 5 (the other four species were studied and the observed isotherms were similar to *I. sagotiana*, data not shown). Among the six species studied only *O. guyanensis*, *S. rubra, T. melinonii*, and *I. sagotiana* TW aerogels clearly show higher specific surface areas than the corresponding NW aerogels. The surface area data are strongly correlated with the mesopore volume.

*S. rubra* TW adsorbed a 60 times larger amount of nitrogen than NW, yielding a surface area of 64.6 $m^2\ g^{-1}$ for TW and 2.6 $m^2\ g^{-1}$ for NW (Table 1). A similar difference has also been observed in species with a thick G-layer such as chestnut (Clair *et al.*, 2008) or poplar (B Clair, unpublished data). However, a large range of specific surface areas (from 3 $m^2\ g^{-1}$ to 65 $m^2\ g^{-1}$) was observed in TW aerogels among the six species, proving that there are large difference in mesopore amounts between the thick and thin G-layers.

### Pore shape and size distribution

According to the IUPAC classification (Sing *et al.*, 1985), the isotherm of *S. rubra* TW is type IV (Fig. 1) with a H3 type hysteresis loop (Fig. 2), indicating the presence of mesopores between the cellulose microfibrils or in the matrix forming slit-shaped pores with a non-uniform size. The isotherm of *I. sagotiana* TW (as well as the other four species) is intermediate between type IV and type II, indicating the presence of large mesopores with a broad size distribution that continues into the macropore domain. The hysteresis loop is very narrow, the adsorption and desorption branches being almost vertical and nearly parallel above 0.8 relative pressure, confirming the presence of a significant outer surface.

The peak pore sizes estimated from the adsorption and desorption are listed in Table 1. Examples of pore volume

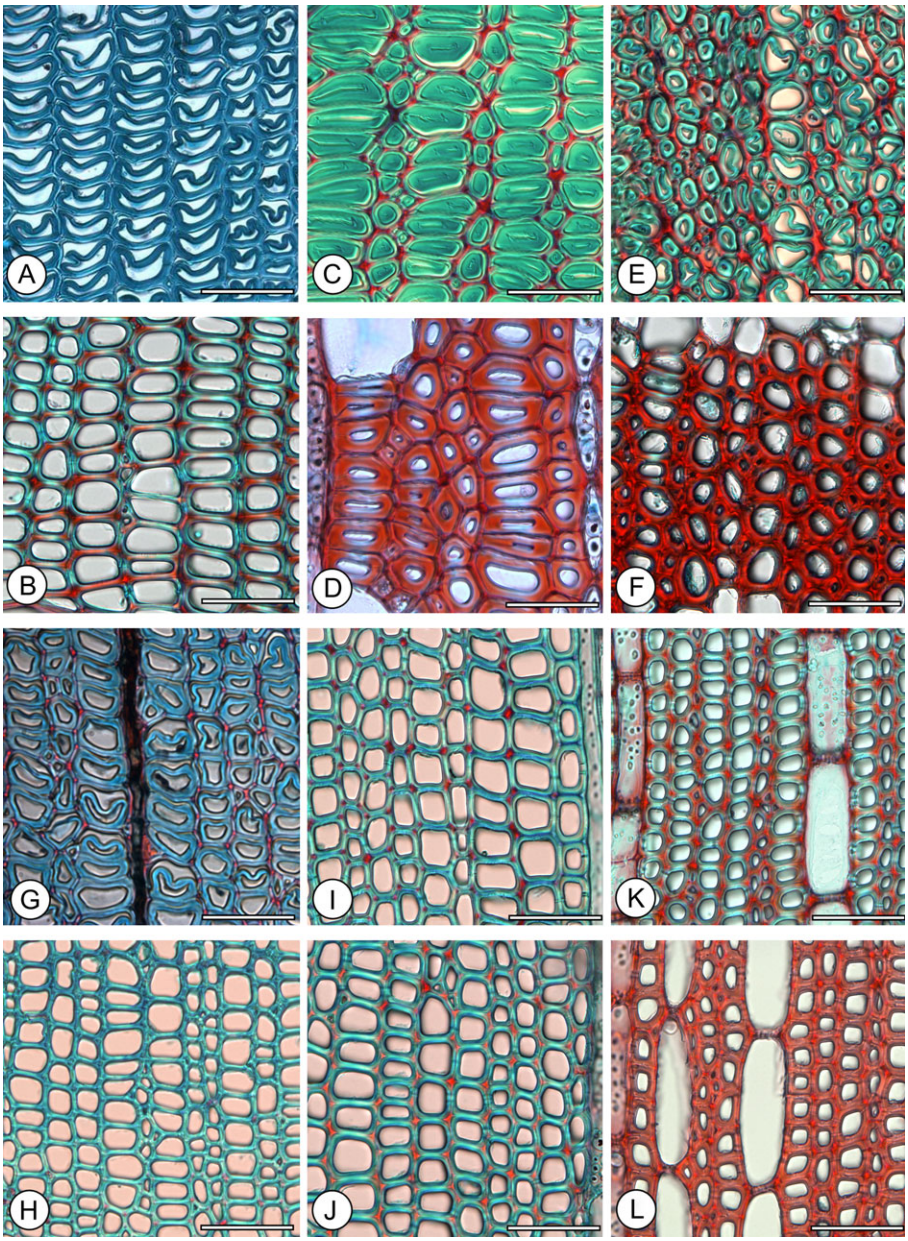


**Fig. 4.** Transverse sections of tension wood and normal wood in six species stained with safranin/fast green. (A, B) *Ocotea guyanensis*. (C, D) *Sextonia rubra*. (E, F) *Inga alba*. (G, H) *Tachigali melinonii*. (I, J) *Virola michelii*. (K, L) *Iryanthera sagotiana*. (A, C, E, G, I, K) Tension wood, (B, D, F, H, J, L) normal wood. Scale bars=50 μm. A G-layer is detected in images (A), (C), (E), and (G) from its swollen aspect and its detachment from the $S_2$ layer. (C) Thick G-layer; (A, E, G) thin G-layer; (I, K) tension wood without a G-layer. In *T. melinonii*, a thin G-layer was observed but it was sparse on the wood sample.

distributions against pore diameter are plotted in Fig. 6 for *S. rubra* and *I. sagotiana* TW aerogels. All the samples present broad pore size distributions, measured both on the adsorption and desorption branches of the isotherms. The sharp peak between 4 nm and 5 nm on the desorption branch is a typical artefact due to the tensional instability of the $N_2$ meniscus (Trens *et al.*, 2005). Pore size distribution determined from the adsorption branch of the isotherm corresponds to the cavity size, while that of the desorption branch corresponds to the throat size of a pore (Groen and Pérez-Ramirez, 2004). Thus, comparing the adsorption and desorption pore size distribution leads to information about the pore shapes. For *S. rubra* and *O. guyanensis* aerogels, the pores have an ink-bottle shape with pore cavities that are less than twice the diameter of the throats. The pore size distribution of *I. alba* suggests pores with a nearly constant diameter. For *V. michelii* (as well as *I. sagotiana* and *T. melinonii*) aerogels, the pore size measured on the adsorption branch is smaller than the pore size measured on the desorption branch. This behaviour indicates that the usual correlations between condensation pressure and pore size do not apply to the geometry of the measured pores. This effect, albeit infrequent, is far from being unprecedented and has been observed in adsorbents with highly connected

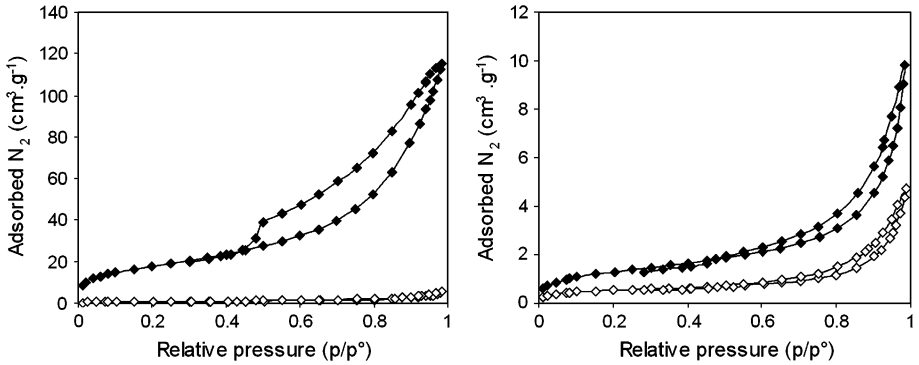


**Fig. 5.** $N_2$ adsorption–desorption at 77 K isotherms of *Sextonia rubra* (left) and *Iryanthera sagotiana* (right). Filled symbols, tension wood; open symbols, normal wood.

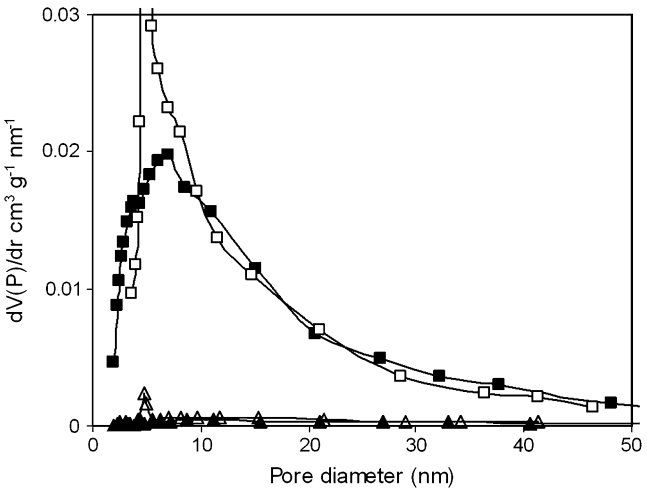


**Fig. 6.** Pore size distributions for *Sextonia rubra* (squares) and *Iryanthera sagotiana* (triangles) tension wood. Filled symbols, adsorption; open symbols, desorption.

tridimensional pore systems (Fan *et al.*, 2001) and can be attributed to funnel-like pores with a wide opening, which decreases the activation energy of condensation.

All porosity parameters observed in *S. rubra* correspond to what was described for the chestnut G-layer (Clair *et al.*, 2008) and also observed for the poplar G-layer (B Clair, unpublished data) which also present thick G-layers; i.e. an isotherm of type IV, presenting a typical hysteresis loop of mesoporous adsorbents with a pore size diameter between 2 nm and 50 nm (Clair *et al.*, 2008) with a maximum around 6 nm. *S. rubra* was the only sample of the present study with a thick G-layer. Other samples with a thin G-layer, like *O. guyanensis* and *T. melinonii*, present an extremely low mesopore volume, suggesting that not all G-layers present a porosity which can be easily stabilized by supercritical drying.

In the case of *I. alba*, another species with a thin G-layer in TW, the mesoporosity of NW has been measured at a much higher level than that of any other NW, and was even slightly higher than that of its TW. Moreover, the shape of the pores seems to be different from the ink-bottle pores of chestnut and *S. rubra* TW.

In species without a G-layer, mesoporosity was low and at the same level in NW and TW (a similar observation was made on *Simarouba amara*; B Clair, unpublished data). Moreover, for *V. michelii*, *I. sagotiana*, and *T. melinonii* the shape of the pores seems to correspond to a pore system more accessible than the interfibrillar mesoporosity of chestnut TW (Clair *et al.*, 2008).

## Discussion

This study shows the ability of the nitrogen adsorption–desorption isotherm method to characterize mesoporosity in wood. It appears that mesoporosity can always be detected in never-dried wood samples. The number of pores can be very different between the samples and the structures of the pore networks are also different. In wood with a thick G-layer, the large amount of mesopores can easily be attributed to the G-layer itself and provides indications about the nature of pores. Pores have ink-bottle shapes with a pore body size distributed around 6–11 nm and a pore mouth around 6 nm and can be attributed to cavities between macrofibrils. In wood without a G-layer, the mesopore volume is very small and the narrow hysteresis could correspond to a network of large-mouth funnel pores. *I. alba*, a species with a thin G-layer and an intermediate mesopore volume, presents an intermediate width of the hysteresis loop, which could be attributed to the simultaneous presence of both pore systems, the one related to the G-layer and the one typical of woods without a G-layer.

The G-layer is known to be composed of pectin and hemicelluloses such as xyloglucan and (1,4)-β-galactan (Nishikubo *et al.*, 2007; Arend, 2008; Bowling and Vaughn, 2008; Mellerowicz *et al.*, 2008). These components would also be present in other cell wall layers (in NW cell wall) in a highly hydrated state allowing it to keep its mesoporosity. The pit membrane, which is known to be composed of pectin gel (Zwieniecki *et al.*, 2001; Van Ieperen, 2007), would also be a good candidate for the place where mesoporosity can be concentrated. In *I. alba*, where the mesoporosity has been measured higher in NW than in TW, axial parenchyma could be susceptible to contain such

mesoporosity since its abundance was measured around 40% in NW and 20% in TW.

This study provides new insights into the understanding of the G-layer since it confirms that major differences between species can be observed in TW fibre secondary walls. All these species are able to produce high tensile stress but their anatomy and nanostructure can differ widely. The following conclusions can be drawn. (i) TW that does not develop a G-layer does not contain a mesoporosity significantly higher than the NW. (ii) TW developing a G-layer can be separated into two classes, a thin G-layer presenting little mesoporosity and a thick G-layer showing a high mesoporosity. The fact that mesoporosity is observable only when the G-layer is thick leads to a new open question. Is the G-layer thick merely because of its high mesoporosity allowing it to remain highly hydrated in a swollen state? In that case, the total amount of cellulose would be not so different in a swollen G-layer compared to a thin G-layer. This would explain why both TW types can produce similar high tensile growth stresses. It would then be interesting to follow the maturation process of these woods and detect the swelling or shrinkage in the gel, which is currently suspected as being responsible for the growth stress generation in TW.

It is quite likely that several mechanisms contribute to the generation of high tensile stress to maintain the vertical orientation of the main stem. The characterization of microstructural features of different woods and their correlation with mechanical parameters are a first step towards an assessment of the possible mechanisms. Then we can hypothesize that mechanisms differ from species to species and, in some cases, are not directly linked to mesoporosity. An alternative hypothesis would be a common mechanism, but apparent mesoporosity would be a residual state of the maturation process that was later hidden in some species.

## Acknowledgements

The authors wish to thank Dr K Abe for his assistance in collecting the tropical wood species. Thanks also go to Dr T Alméras for a critical review of the manuscript. The study was performed in the framework of the ANR project 'Woodiversity'. The first author was supported by the Chinese Government Scholarship Program.

## References

**Arend M.** 2008. Immunolocalization of (1,4)-β-galactan in tension wood fibers of poplar. *Tree Physiology* **28,** 1263–1267.

**Barrett EP, Joyner LG, Halenda PH.** 1951. The determination of pore volume and area distributions in porous substances. *Journal of the American Chemical Society* **73,** 373–380.

**Bowling AJ, Vaughn KC.** 2008. Immunocytochemical characterization of tension wood: gelatinous fibers contain more than just cellulose. *American Journal of Botany* **95,** 655–663.

**Brunauer S, Emmett PH, Teller E.** 1938. Adsorption of gases in multimolecular layers. *Journal of the American Chemical Society* **60,** 309–319.

**Cansell F, Aymonier C, Loppinet-Serani A.** 2003. Review on materials science and supercritical fluids. *Current Opinion in Solid State and Materials Science* **7,** 331–340.

**Clair B, Gril J, Baba K, Thibaut B, Sugiyama J.** 2005*a*. Precautions for the structural analysis of the gelatinous layer in tension wood. *IAWA Journal* **26,** 189–195.

**Clair B, Gril J, Di Renzo F, Yamamoto H, Quignard F.** 2008. Characterization of a gel in the cell wall to elucidate the paradoxical shrinkage of tension wood. *Biomacromolecules* **9,** 494–498.

**Clair B, Ruelle J, Beauchêne J, Prevost MF, Fournier M.** 2006. Tension wood and opposite wood in 21 tropical rain forest species. 1. Occurrence and efficiency of the G-layer. *IAWA Journal* **27,** 329–338.

**Clair B, Ruelle J, Thibaut B.** 2003. Relationship between growth stress, mechanical-physical properties and proportion of fibre with gelatinous layer in chestnut (*Castanea sativa* Mill.). *Holzforschung* **57,** 189–195.

**Clair B, Thibaut B.** 2001. Shrinkage of the gelatinous layer of poplar and beech tension wood. *IAWA Journal* **22,** 121–131.

**Clair B, Thibaut B, Sugiyama H.** 2005*b*. On the detachment of the gelatinous layer in tension wood fiber. *Journal of Wood Science* **51,** 218–221.

**Côté WAJ, Day AC, Timell TE.** 1969. A contribution to the ultrastructure of tension wood fibers. *Wood Scence and Technology* **3,** 257–271.

**Dadswell HE, Wardrop AB.** 1955. The structure and properties of tension wood. *Holzforschung* **9,** 97–104.

**Fan J, Yu CZ, Wang LM, Tu B, Zhao DY, Sakamoto Y, Terasaki O.** 2001. Mesotunnels on the silica wall of ordered SBA-15 to generate three-dimensional large-pore mesoporous networks. *Journal of the American Chemical Society* **123,** 12113–12114.

**Fang CH, Clair B, Gril J, Alméras T.** 2007. Transverse shrinkage in G-fibers as a function of cell wall layering and growth strain. *Wood Science and Technology* **41,** 659–671.

**Fang CH, Clair B, Gril J, Liu SQ.** 2008. Growth stresses are highly controlled by the amount of G-layer in poplar tension wood. *IAWA Journal* **29,** 237–246.

**Fisher JB, Stevenson JW.** 1981. Occurrence of reaction wood in branches of dicotyledons and its role in tree architecture. *Botanical Gazette* **142,** 82–95.

**Galarneau A, Desplantier D, Dutartre R, Di Renzo F.** 1999. Micelle-templated silicates as a test-bed for methods of pore size evaluation. *Microporous and Mesoporous Materials* **27,** 297–308.

**Goswami L, Dunlop JWC, Jungnikl K, Eder M, Gierlinger N, Coutand C, Jeronimidis G, Fratzl P, Burgert I.** 2008. Stress generation in the tension wood of poplar is based on the lateral swelling power of the G-layer. *The Plant Journal* **56,** 531–538.

**Gregg SJ, Sing KSW.** 1982. *Adsorption, surface area and porosity*. London: Academic Press, 218–228.

**Groen JC, Pérez-Ramirez J.** 2004. Critical appraisal of mesopore determination by adsorption analysis. *Applied Catalysis A: General* **268,** 121–125.

**Isebrands JG, Bensend DW.** 1972. Incidence and structure of gelatinous fibers within rapid-growing eastern cottonwood. *Wood Fiber Science* **4,** 61–71.

**Jullien D, Gril J.** 2008. Growth strain assessment at the periphery of small-diameter trees using the two-grooves method: influence of operating parameters estimated by numerical simulations. *Wood Science and Technology* **42,** 551–565.

**Mellerowicz EJ, Immerzeel P, Hayashi T.** 2008. Xyloglucan: the molecular muscle of trees. *Annals of Botany* **102,** 659–665.

**Nishikubo N, Awano T, Banasiak A, *et al*.** 2007. Xyloglucan *endo*-transglycosylase (XET) functions in gelatinous layers of tension wood fibers in poplar: a glimpse into the mechanism of the balancing act of trees. *Plant and Cell Physiology* **48,** 843–855.

**Onaka F.** 1949. Studies on compression and tension wood. In: *Wood research*. Bulletin of the Wood Research Institute, Kyoto University, Japan **24,** 1–88.

**Pierre AC, Pajonk GM.** 2002. Chemistry of aerogels and their applications. *Chemical Reviews* **102,** 4243–4266.

**Quignard F, Valentin R, Di Renzo F.** 2008. Aerogel materials from marine polysaccharides. *New Journal of Chemistry* **32,** 1300–1310.

**Rouquerol F, Rouquerol J, Sing K.** 1999. *Adsorption by powders and porous solids: principles, methodology and applications*. San Diego: Academic Press, 439–467.

**Ruelle J, Clair B, Beauchêne J, Prévost MF, Fournier M.** 2006. Tension wood and opposite wood in 21 tropical rain forest species. 2. Comparison of some anatomical and unltrastuctural criteria. *IAWA Journal* **27,** 341–376.

**Ruelle J, Yamamoto H, Thibaut B.** 2007. Growth stresses and cellulose structural parameters in tension and normal wood from three tropical rainforest angiosperms species. *Bioresources* **2,** 235–251.

**Sing KSW, Everett DH, Haul RAW, Moscou L, Pierotti RA, Rouquerol J, Siemienewska T.** 1985. Reporting physisorption data for gas–solid systems. *Pure and Applied Chemistry* **57,** 603–619.

**Trénard Y, Guéneau P.** 1975. Relations entre contraintes de croissance longitudinales et bois de tension dans le hêtre (*Fagus sylvatica* L.). *Holzforschung* **29,** 217–223.

**Trens P, Tanchoux N, Galartneau A, Brunel D, Fubini B, Garrone E, Faula F, Di Renzo F.** 2005. A macrothermodynamic approach to the limit of reversible capillary condensation. *Langmuir* **21,** 8560–8564.

**Valentin R, Molvinger K, Quignard F, Di Renzo F.** 2005. Methods to analyse the texture of alginate aerogel microspheres. *Macromolecular Symposia* **222,** 93–101.

**Van Ieperen W.** 2007. Ion-mediated changes of xylem hydraulic resistance *in planta*: fact or fiction? *Trends in Plant Science* **12,** 137–142.

**Wardrop AB.** 1964. The reaction anatomy of arborescent angiosperms. In: Zimmermann MH, ed. *The formation of wood in forest trees*. New York: Academic Press, 405–456.

**Yamamoto H, Abe K, Arakawa Y, Okuyama T, Gril J.** 2005. Role of the gelatinous layer (G-layer) on the origin of the physical properties of the tension wood of *Acer sieboldianum*. *Journal of Wood Science* **51,** 222–233.

**Yoshida M, Okuyama T.** 2002. Techniques for measuring growth stress on the xylem surface using strain and dial gauges. *Holzforschung* **56,** 461–467.

**Zwieniecki MA, Melcher PJ, Holbrook NM.** 2001. Hydrogel control of xylem hydraulic resistance in plants. *Science* **291,** 1059–1062.